

# A Feedback Control Framework for Personalization of Coronary Flow Simulations during Rest and Hyperemia

Puneet Sharma<sup>1</sup>, Lucian Itu<sup>2,3</sup>, Xudong Zheng<sup>1</sup>, Ali Kamen<sup>1</sup>, Constantin Suciuc<sup>2,3</sup>, Dorin Comaniciu<sup>1</sup>

**Abstract**—We introduce a Computational Fluid Dynamics (CFD) based method for performing patient-specific coronary hemodynamic simulations under two conditions: at rest and during drug-induced hyperemia. The proposed method is based on a novel estimation procedure for determining the boundary conditions from non-invasively acquired patient data at rest. A multi-variable feedback control framework ensures that the simulated mean arterial pressure and the flow distribution matches the estimated values for an individual patient during the rest state. The boundary conditions at hyperemia are derived from the respective rest-state values via a transfer function that models the vasodilation phenomenon. Simulations are performed on a coronary tree where a 65% diameter stenosis is introduced in the left anterior descending (LAD) artery, with the boundary conditions estimated using the proposed method. The results demonstrate that the estimation of the hyperemic resistances is crucial in order to obtain accurate values for pressure and flow rates. Sensitivity analysis of the model shows that the trans-stenotic pressure drop is most sensitive with respect to the systolic and diastolic cuff pressures, while the left ventricular mass has the highest influence on the predicted Fractional Flow Reserve (FFR) value.

## I. INTRODUCTION

In recent years, several methods based on Computational Fluid Dynamics (CFD) have been proposed for non-invasive estimation of coronary circulation [1], [2], [3], with promising results. The main challenges for such methods are the lack of patient-specific data including anatomy and boundary conditions, inefficient multi-scale coupling and the large-scale computational resources required for the complex simulations (often requiring several hours of simulations on large clusters). These challenges limit the scope of such methods in a routine clinical setting.

In this paper, we propose a method for estimating patient-specific coronary boundary conditions during rest and hyperemia, and a feedback control based system to perform personalized CFD simulations that match the patient's hemodynamic parameters. The method is based on computed hemodynamic parameters acquired non-invasively during the rest state.

The procedure is as follows: first the rest boundary conditions are determined, followed by a computation of the hyperemic boundary conditions. Next, a feedback control system is used to perform a simulation that matches the rest

state, and finally, after setting up the hyperemic boundary conditions, the arterial model is taken out of the control loop and the simulation corresponding to the hyperemic state is performed (see Figure 1). The methods were tested with a reduced-order model, which we introduced in [4].

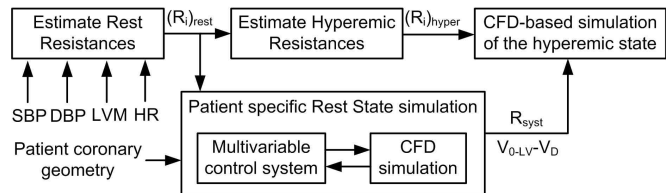


Fig. 1. Flowchart of the proposed method

## II. METHOD

For an accurate simulation of a patients coronary blood-flow, two key requirements for CFD-based methods are - (a) anatomical model of the coronary vessel tree and (b) the boundary conditions at the inlet and outlets. Recent advances in medical image processing have addressed the former by employing manual, semi-automatic or fully-automatic algorithms for multi-modality image segmentation and surface mesh generation, but there has been considerably less focus on the latter. Most of the work on coupling patient-specific boundary conditions for coronary simulations has relied on population-wide average values (thereby rendering it incapable of estimating hemodynamic quantities for an individual patient), or on invasively determined pressure or flow-rate values [1], [3].

### A. Estimation of Boundary Conditions at Rest State

Since the region of interest, namely the coronary vessel tree is part of the larger circulation system, the inlet and outlet boundary conditions should be chosen such that they adequately model the proximal and distal phenomenon of the patients circulation. For the coronary outlets, several models have been proposed [5], [6] which take into account the effect of the myocardial contraction on the flow. These lumped models are usually composed of a set of resistances and compliances, which represent the micro-vascular beds. The compliance influences the transient waveform, while the mean value is affected only by the resistance. Since the key diagnostic indexes (such as FFR and CFR) are based on average quantities over the cardiac cycle, the boundary condition estimation is limited to correctly determining the resistance values at each outlet, which is defined as the ratio

<sup>1</sup>Siemens Corporation, Corporate Research & Technology, Princeton, New Jersey, United States. Emails: {sharma.puneet, xudong.zheng, ali.kamen, dorin.comaniciu}@siemens.com

<sup>2</sup>Transilvania University of Brasov, Brasov, Romania. Email: lucian.itu@unitbv.ro

<sup>3</sup>Siemens Corporate Technology, Brasov, Romania. Email: constantin.suciuc@siemens.com

of the pressure to the flow through that outlet. Mean arterial pressure (MAP) is constant in healthy epicardial arteries and can be estimated by systolic, diastolic cuff blood pressures (SBP and DBP), and the heart rate [7]:

$$MAP = DBP + \left[ \frac{1}{3} + (HR \times 0.0012) \right] (SBP - DBP)$$

Coronary flow depends on the oxygen demand of the heart and since oxygen extraction in the coronary capillaries is close to maximum levels even at rest state, the increased metabolic need can be satisfied only through an increased flow, hence coronary flow is proportional to the oxygen demand. It is difficult to quantify oxygen demand and consumption in the coronaries through non-invasive measurements. Several methods for estimating oxygen consumption from mechanical variables have been proposed in the past, with heart rate as a primary determinant of oxygen consumption. The second major determinant is pressure (pressure generation costs more oxygen than muscle shortening, i.e. flow). The most widely used index for estimating the myocardial oxygen consumption is the rate-pressure product [8], according to which,

$$q_{rest} = 8 \times \{ [7 \times 10^{-4} (HR \cdot SBP)] - 0.4 \} \text{ ml/min/100g} \quad (1)$$

To determine the absolute value of resting flow ( $Q_{rest}$ ), resting perfusion is multiplied with total myocardial mass. In normal hearts, the left ventricle typically represents two-thirds of the total mass, i.e.  $Q_{rest} = q_{rest} \times 1.5 \times M_{LV}$ . Hence total coronary resistance can be computed as  $R_{cor} = MAP/Q_{rest}$ . The value  $M_{LV}$  is estimated from CT images by myocardial segmentation, as described in [9].

The next step is to distribute the total resistance to the various lumped models at the outlets. To do this, we use Murray's law [10], which states that the energy required for blood flow and the energy needed to maintain the vasculature is assumed minimal and hence,  $Q_i \sim k \cdot r_i^3$ , where  $k$  is a constant and  $r$  is the radius of the vessel. A value of 3 for the power coefficient has been suggested through the observed invariability of wall shear stress (rate) when flow rate varies substantially [11]. Next, the absolute resting flow, which is the sum of all outlet flows, is written as  $Q_{rest} = \sum_{i=1}^n k \cdot r_i^3 = \sum_{i=1}^n Q_i$ , and the flow through a particular outlet is determined by

$$\frac{Q_i}{Q_{rest}} = \frac{k \cdot r_i^3}{\sum_{j=1}^n k \cdot r_j^3} \Rightarrow Q_i = Q_{rest} \cdot \frac{r_i^3}{\sum_{j=1}^n r_j^3} \quad (2)$$

Therefore, the terminal resistances can be determined by,

$$R_i = \frac{MAP}{Q_i} = MAP \cdot \frac{\sum_{j=1}^n r_j^3}{Q_{rest} \cdot r_i^3} \quad (3)$$

### B. Estimation of Boundary Conditions at Hyperemia

Intracoronary and intravenously drug-induced hyperemia lead to similar decreases in micro-vascular resistances [12]. Intravenous administration of adenosine leads to a slight increase in heart rate and decrease in blood pressure [13]. For a simulation, the effect of intracoronary vasodilators

can be extended infinitely and it minimally influences the heart rate and blood pressure [13]. Adenosine leads to an increase in coronary flow velocity of around 4.5 for normal, healthy subjects (with no coronary artery disease) [12]. Since blood pressure decreases slightly during hyperemia, a 4.5-fold increase in flow does not mean a 4.5-fold decrease in coronary resistance. A total coronary resistance index can be computed (TCRI), which is equal to:

$$TCRI = \left( \frac{MAP_{hyper}}{Q_{hyper}} / \frac{MAP_{rest}}{Q_{rest}} \right) = \frac{(R_{cor})_{hyper}}{(R_{cor})_{rest}} \quad (4)$$

A mean value of  $TCRI = 0.22$  has been obtained during various studies. It increases from 0.22, for HR less than 75bpm, to 0.26, for a heart rate of 100bpm, and to 0.28 for a heart rate of 120bpm [14]. Therefore, the following relationship can be derived to obtain a HR corrected TCRI:

$$TCRI_{corr} = \begin{cases} 0.0016 \cdot HR + 0.1 & \text{for } HR \leq 100 \text{ bpm;} \\ 0.001 \cdot HR + 0.16 & \text{for } HR > 100 \text{ bpm.} \end{cases} \quad (5)$$

Finally, hyperemic micro-vascular resistances are computed by  $(R_i)_{hyper} = (R_i)_{rest} \cdot TCRI$ , where  $(R_i)_{rest}$  is the value from (3).

### C. Feedback Control System

In order to accurately evaluate coronary diagnostic indexes, the goal of a CFD simulation is to obtain the same average pressure and flow rates as those obtained if the patient were in the rest/drug-induced hyperemia. Once the rest-state outlet resistances have been determined (Section II-A), the next step is to perform the CFD simulation at the rest-state, and ensure that the results match the patient data acquired non-invasively.

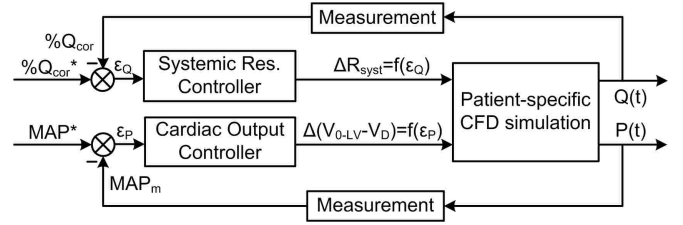


Fig. 2. Multivariable feedback control system used during the rest state simulation

To ensure this, we use a feedback control system (Figure 2), which estimates the optimal values for the control signal (i.e. the free parameters of the model). We chose two free parameters (a) the systemic resistance at the aorta outlet ( $R_{syst}$ ) and (b) the total cardiac output (which is modulated by the difference between initial LV volume and dead volume,  $[V_{0-LV} - V_D]$ ). The estimation is performed under the constraint that the results of the CFD simulation match the reference values (measured patient data). Note that the coronary outlet resistances are not changed during this process. The two reference values are: and the total coronary flow as a percent of the cardiac output ( $\%Q_{cor}^*$ ) and the mean pressure ( $MAP^*$ ). Since the resting coronary

flow is approximately 4-5% of the total cardiac output [13] a reference value of 4.5% is used.

We use a Proportional-Integral-Derivative (PID) controller, where the control signal  $u(t)$  is given by,

$$u(t) = K_p \epsilon(t) + K_I \int_0^t \epsilon(\tau) d\tau + K_D \frac{d}{dt} \epsilon(t), \quad (6)$$

where  $K_p$ ,  $K_I$  and  $K_D$  are the gains, and  $\epsilon$  is the error between the measured and the reference value. We designed a PI controller for the systemic resistance control ( $K_P = 40.1$ ,  $K_I = 2.6$ ), and a PID controller for the cardiac output control ( $K_P = 0.876$ ,  $K_I = 0.20372$ ,  $K_D = 0.9417$ ). Note that the goal of the proposed method is to reach a steady-state and accurately match the patient-specific steady-state, and not necessarily model the transient aspects.

Once the CFD-controller loop has converged, optimal values of  $R_{syst}$  and  $[V_{0-LV} - V_D]$  are available. The next step is to perform the CFD simulations at hyperemia. To do this, the control loop is switched off, the rest outlet resistances are substituted by the hyperemic resistances ( $(R_i)_{hyper}$ ), together with the optimal values of  $R_{syst}$ , and  $[V_{0-LV} - V_D]$ . The CFD simulation during hyperemia is run until the pressure and flow rates converge.

### III. RESULTS

The method described in Section II was tested using a reduced-order patient-specific model. The anatomical model of the coronary vessels was obtained from Coronary CT scans by image segmentation, centerline and lumen extraction, as described in [4]. For the CFD simulation, proximal vessels were modeled as axi-symmetric 1D segments, while the micro-vascular beds were represented by lumped models [6] (Figure 3). An artificial 65% diameter stenosis with a length of 1.0 cm was introduced in the LAD. For the CFD simulation, the stenosis was modeled as described in [15]. The coronary tree is coupled to the aorta and a heart model (varying elastance model [4]) is used to provide the inlet boundary condition. If only the coronaries were modeled, then either time-varying flow or pressure would be needed at inflow, none of which is available non-invasively.

In Sections II-A and II-B the total outflow resistances have been determined, while the lumped coronary models are composed of four different resistances. The first resistance is equal to the characteristic resistance in order to minimize the reflections, while the third and fourth resistances represent the micro-vascular venous and venous resistances which are considered constant. Thus the micro-vascular arterial resistance is determined as difference between the total and the three other resistances. Note that the average pressure and flow depend on total resistance and not on its distribution to the individual resistances.

Figure 4 displays the evolution of the two controlled variables ( $MAP$  and  $\%Q_{cor}$ ) and the inputs ( $R_{syst}$  and  $[V_{0-LV} - V_D]$ ) during a simulation performed with the base values:  $HR = 60 \text{ bpm}$ ,  $SBP = 140 \text{ mmHg}$ ,  $DBP = 100 \text{ mmHg}$ ,  $LVM = 250 \text{ gm}$ ,  $n = 3$ . Each plot is divided into three phases:

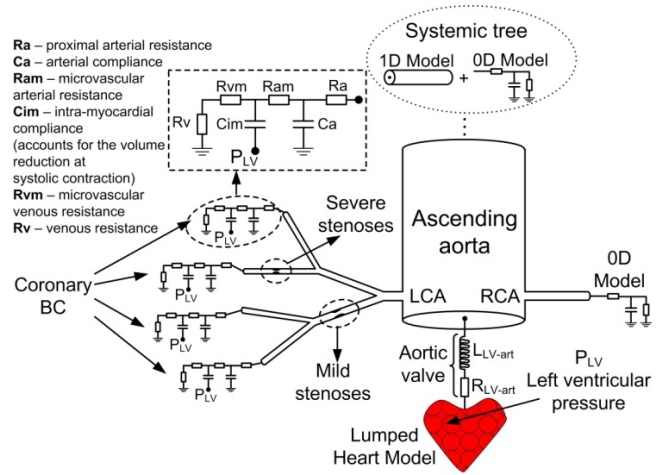


Fig. 3. Reduced-order model of the coronary circulation

- ① initialization phase,
- ② rest-state simulation phase (with control system based estimation), and
- ③ hyperemic state simulation phase.

During phase ②, the values converge to the reference values estimated for the rest-state of the patient (see Figure 4). In phase ③, the inputs remain constant (feedback loops are not active), the aortic pressure decreases while the percentage coronary flow increases (as is observed in hyperemia).

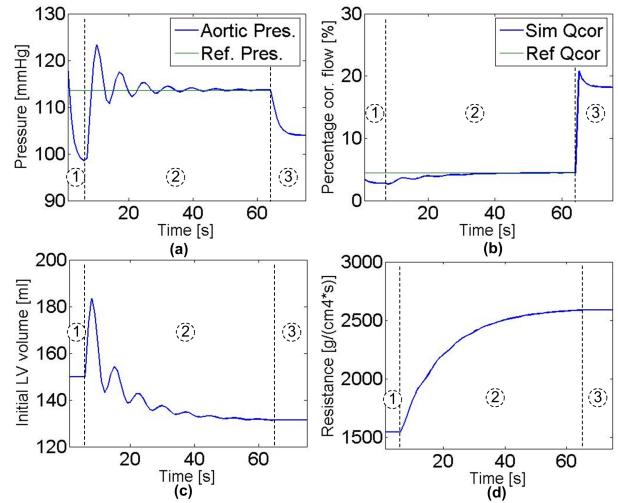


Fig. 4. Evolution of (a) Aortic pressure, (b) % coronary flow, (c) Initial LV volume, (d) Systemic resistance

Sensitivity analysis was performed for the four input parameters of the CFD simulation:  $HR$ ,  $SPB$  and  $DBP$  (taken together, since  $MAP$  is the actual input),  $LVM$  and  $n$ . Each input parameter was varied by  $\pm 10\%$ ,  $\pm 20\%$  and  $\pm 30\%$  (except  $n$ , where only  $\pm 10\%$  and  $\pm 20\%$  variations were done).  $SBP$  and  $DBP$  were varied simultaneously by the same percentage.

Figure 6 shows the results of the sensitivity analysis for the trans-stenotic pressure drop ( $\Delta P$ ) and  $FRR = P_d/P_a$ .



Fig. 5. Patient-specific coronary geometry

The highest sensitivity for  $\Delta P$  is with respect to the cuff pressures, followed by  $LVM$ . For  $FFR$ , the highest sensitivity is with respect to the  $LVM$ , followed by  $HR$ . In both cases, the power coefficient has minimal influence.

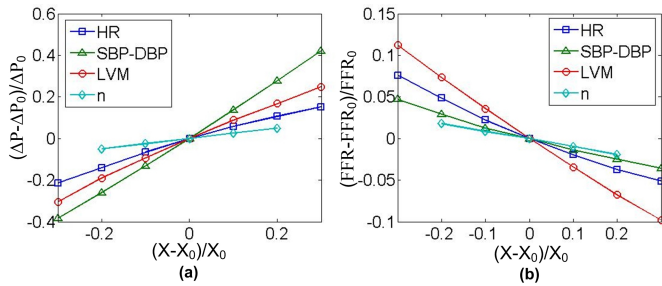


Fig. 6. (a) Sensitivity analysis of the trans-stenotic pressure drop, (b) Sensitivity analysis of the ratio  $P_d/P_a$ , where  $X$  refers to  $HR$ ,  $SBP$ - $DBP$ ,  $LVM$  and  $n$

To further demonstrate the need for accurate outlet boundary condition estimation, a sensitivity analysis with respect to the hyperemic resistances was performed, where  $(R_i)_{hyper}$  was perturbed by  $\pm 10\%$ ,  $\pm 20\%$  and  $\pm 30\%$ . The results for  $\Delta P$  and  $FFR$  are shown in Table I. The results show that it is crucial to accurately determine the rest and hyperemic micro-vascular resistance of each outlet. For the given case,  $FFR$  value varies between 0.628 and 0.784, an interval which intersects the cut-off value used in clinical practice.

TABLE I

EFFECT OF CHANGE IN HYPEREMIC RESISTANCE ON  $\Delta P$  AND  $P_d/P_a$ .

Pressure : mmHg, resistance :  $g/(cm^4s)$ , flow : ml/s.

$R_{hyper}$	$P_a$	$P_d$	$Q$	$\Delta P$	$P_d/P_a$
7579 (-30%)	100.01	62.79	2.11	37.22	0.628
8661 (-20%)	101.64	67.55	1.99	34.09	0.664
9744 (-10%)	102.97	71.67	1.88	31.30	0.696
10827 (0%)	104.01	75.21	1.77	28.80	0.723
11919 (+10%)	105.03	78.40	1.68	29.8	0.746
12993 (+20%)	105.83	81.17	1.60	24.66	0.766
14076 (+30%)	106.54	83.62	1.52	22.92	0.784

#### IV. CONCLUSIONS

We have introduced a method for estimating patient-specific coronary boundary conditions (at rest and hyperemia) together with a feedback control system to ensure that

CFD-based simulation match the patient-specific coronary pressure and flow. The main advantages of this approach are that it is based on parameters, which are acquired non-invasively during the rest state, and can be used for full-order or reduced-order simulations. Further, it can be used to assess coronary diagnostic indexes which are based solely on the hyperemic state (e.g.  $FFR$ ) or based on both rest and hyperemic state (e.g.  $CFR$ ).

The main limitations of the proposed method are - (a) patients with rest angina were excluded since (1) may not be valid (rest flow does not meet the oxygen demand), and (b) patients with micro-vascular disease and hypertension should be modeled separately, since (5) would be no longer valid.

#### REFERENCES

- [1] Y. Huo and G. S. Kassab, "A hybrid one-dimensional/womersley model of pulsatile blood flow in the entire coronary arterial tree," *American Journal of Physiology - Heart and Circulatory Physiology*, vol. 292, no. 6, pp. H2623–H2633, 2007.
- [2] H. Kim, I. Vignon-Clementel, J. Coogan, C. Figueroa, K. Jansen, and C. Taylor, "Patient-specific modeling of blood flow and pressure in human coronary arteries," *Annals of Biomedical Engineering*, vol. 38, pp. 3195–3209, 2010.
- [3] A. van der Horst, F. L. Boogaard, M. Rutten, and F. van de Vosse, "A 1d wave propagation model of coronary flow in a beating heart," *Proc. of the Summer Bioengineering Conference, Farmington, PA, USA*, 2011.
- [4] L. Itu, P. Sharma, V. Mihalef, A. Kamen, C. Suciuc, and D. Comaniciu, "A patient-specific reduced-order model for coronary circulation," in *IEEE International Symposium on Biomedical Imaging (to appear)*, May 2012.
- [5] P. Bruinsma, T. Arts, J. Dankelman, and J. A. E. Spaan, "Model of the coronary circulation based on pressure dependence of coronary resistance and compliance," *Basic Research in Cardiology*, vol. 83, pp. 510–524, 1988.
- [6] S. Mantero, R. Pietrabissa, and R. Fumero, "The coronary bed and its role in the cardiovascular system: a review and an introductory single-branch model," *Journal of Biomedical Engineering*, vol. 14, no. 2, pp. 109 – 116, 1992.
- [7] M. Razminia, A. Trivedi, J. Molnar, M. Elbzour, M. Guerrero, Y. Salem, A. Ahmed, S. Khosla, and D. L. Lubell, "Validation of a new formula for mean arterial pressure calculation: The new formula is superior to the standard formula," *Catheterization and Cardiovascular Interventions*, vol. 63, no. 4, pp. 419–425, 2004.
- [8] H. V. Anderson, M. J. Stokes, M. Leon, S. A. Abu-Halawa, Y. Stuart, and R. L. Kirkeeide, "Coronary artery flow velocity is related to lumen area and regional left ventricular mass," *Circulation*, vol. 102, no. 1, pp. 48–54, 2000.
- [9] Y. Zheng, A. Barbu, B. Georgescu, M. Scheuering, and D. Comaniciu, "Four-chamber heart modeling and automatic segmentation for 3-d cardiac ct volumes using marginal space learning and steerable features," *IEEE Trans. Med. Imaging*, vol. 27, no. 11, pp. 1668–1681, 2008.
- [10] C. D. Murray, "The Physiological Principle of Minimum Work: I. The Vascular System and the Cost of Blood Volume," *Proceedings of the National Academy of Sciences of the United States of America*, vol. 12, no. 3, pp. 207–214, 1926.
- [11] A. Kamiya and T. Togawa, "Adaptive regulation of wall shear stress to flow change in the canine carotid artery," *American Journal of Physiology - Heart and Circulatory Physiology*, vol. 239, no. 1, pp. H14–H21, 1980.
- [12] R. Wilson, K. Wyche, B. Christensen, S. Zimmer, and D. Laxson, "Effects of adenosine on human coronary arterial circulation," *Circulation*, vol. 82, no. 5, pp. 1595–1606, 1990.
- [13] N. Pijls and B. de Bruyne, *Coronary Pressure*. Springer, 2000.
- [14] A. McGinn, C. White, and R. Wilson, "Interstudy variability of coronary flow reserve. influence of heart rate, arterial pressure, and ventricular preload," *Circulation*, vol. 81, no. 4, pp. 1319–1330, 1990.
- [15] Y. Huo, M. Svendsen, J. S. Choy, Z.-D. Zhang, and G. S. Kassab, "A validated predictive model of coronary fractional flow reserve," *Journal of The Royal Society Interface*, 2011.